Available online at www.sciencedirect.com
ScienceDirect
Journal of the European Ceramic Society 29 (2009) 481–487
www.elsevier.com/locate/jeurceramsoc

High-temperature fatigue behavior of SiC-coated carbon/carbon composites in oxidizing atmosphere

Chidong Liu *, Laifei Cheng, Xingang Luan, Hui Mei

National Key Laboratory of Thermostructure Composite Materials, P.O. Box 547, Northwestern Polytechnical University, Xi'an, Shaan'xi, 710072, PR China

Received 3 April 2008; received in revised form 13 June 2008; accepted 20 June 2008
Available online 26 July 2008

Abstract

Tensile fatigue-stressed oxidation experiments were conducted at 1300 °C in oxidizing atmosphere to identify the failure modes and degradation mechanism of a SiC-coated carbon/carbon composite. Five peak fatigue stresses were selected between 90 and 150 MPa and the results showed that the higher the applied stress, the shorter the composite life. Electrical resistance of the composite was acquired in real-time. The composite resistance appeared a slight drop in the initial fatigue period and followed by a continuous increase until failure. Both the changes in modulus and resistance revealed the shrinking core mechanism in the fatigue-stressed oxidation experiments. A model was developed based on a half-cylinder oxidation pattern. Simulations were conducted on the basis of this model, and the results agreed with the experimental data fairly well.

Keywords: Carbon/carbon composites; Fatigue; Corrosion; Lifetime; Electrical properties

1. Introduction

Carbon/carbon (C/C) composites have received increasing attention in recent decades due to the superior properties at room as well as elevated temperatures. Many of the high-temperature applications of C/C composites call for thorough understanding of damage development under fatigue loading.

The reactivity of carbon in oxidizing atmospheres at high temperatures is the drawback. Coating is an efficient method for protecting C/C composites from oxidation. SiC ceramic is widely used as a coating to provide protection against oxidation owing to its excellent anti-oxidation properties and good compatibility with C/C composites.[1–4] Because of the thermal expansion mismatch between the SiC coating and C/C substrate, cracks are inevitable.[5,6] These cracks provide paths for oxidizing species to attack the C/C with formation of a cavity below the coating and eventual consumption of the underlying composite. Moreover, once the composite is loaded by tensile stress, cracks of the SiC coating will be widened and probably increase the carbon oxidation rate.[7]

The present work was to investigate the high-temperature fatigue behavior of SiC-coated C/C composites in oxidizing atmosphere. The coupled effect of oxidation and cyclic loading damages on lifetime was discussed and a model was established on the basis of half-cylinder oxidation pattern. The electrical resistance of C/C specimens was acquired in real-time, and thus used to help understanding the mechanical degradation of the composite.

2. Experimental

T-300 carbon fibres (Toray, Japan) were used. The fibre preform was prepared using a layered carbon-cloth braid method. The volume fraction of fibres was about 40%. Thermal gradient chemical vapor infiltration was employed to deposit the carbon matrix, using CH_4 as the precursor. Finally, the specimens were machined from the fabricated composite plate (see Fig. 1 for the detailed specimen dimensions). The density of the as-received composite was $\rho = 1.75\ g/cm^3$. The mean tensile strength and elastic modulus of the specimens were $\sigma_0 = 264.2$ MPa and $E_0 = 67.3$ GPa, respectively. The specimens were further coated with two layers of chemical vapor deposited SiC (deposition temperature is approximately 1100 °C) in order to protect the C/C substrate from oxidation.

* Corresponding author. Tel.: +86 29 88494620; fax: +86 29 88494620.
E-mail address: lcd_tscm@hotmail.com (C. Liu).

0955-2219/$ – see front matter © 2008 Elsevier Ltd. All rights reserved.
doi:10.1016/j.jeurceramsoc.2008.06.014

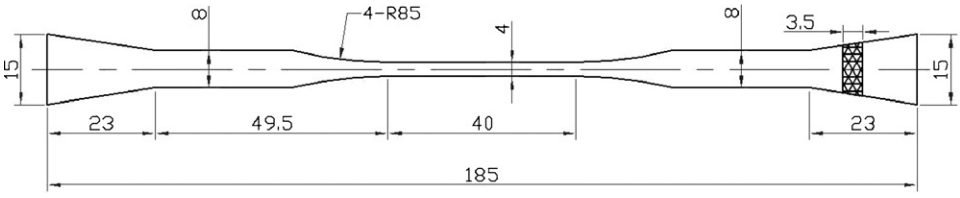

Fig. 1. Drawing of the as-received C/C specimen (all dimensions in mm).

A schematic of the testing equipment is shown in Fig. 2. The chamber temperature was firstly heated to 1300 °C by a graphite heater with the specimen protected by pure argon. After keeping the temperature for 10 min, the atmosphere in the chamber was adjusted to 81.2% Argon, 12.8% water vapor and 6.0% oxygen by mass flow controllers (5850i series of BROOKS, Japan) with the precision of 0.1 ml/min. The atmosphere was changed to pure argon immediately the specimen failed. The time delay in changing atmosphere is less than 10 s, which has little effect on the fracture section morphology.

Fatigue loadings were provided by a servo-hydraulic machine (Model Instron 8801, Instron Ltd., England) under load control at the stress ratio ($\sigma_{min}/\sigma_{max}$) of 0.1 and sinusoidal frequency of $f = 3$ Hz. Maximum stress levels of 90, 105, 120, 135 and 150 MPa were selected. The strain was measured by an extensometer, which was fixed out of the furnace. The strain data was further revised according to the calibration result obtained at room temperature. The detailed calibration process and the data precision are shown in Ref.[8]. The least number of specimens for each test is three. Composite resistance was acquired by a high-accuracy digital multimeter at 100 Hz and saved with logarithmic intervals in order to reduce the data volume. The microstructures of specimens were observed by scanning electron microscope (SEM, JSM-6700F).

3. Results

3.1. Fatigue life of the composite

The fatigue life of the SiC-coated C/C composite at 1300 °C in oxidizing atmosphere is shown in Fig. 3 (solid square dots) as a function of peak stress. The fatigue life decreases as the peak fatigue stress increases. For C/C composites, the fatigue limit at room temperature is about 90% of the tensile strength.[9,10] In the present experiments, all specimens fractured even at much lower stresses than the fatigue limit at room temperature. It is believed that the oxidizing atmosphere is responsible for the short-life at low stresses. If the peak stress is higher than the fatigue limit,

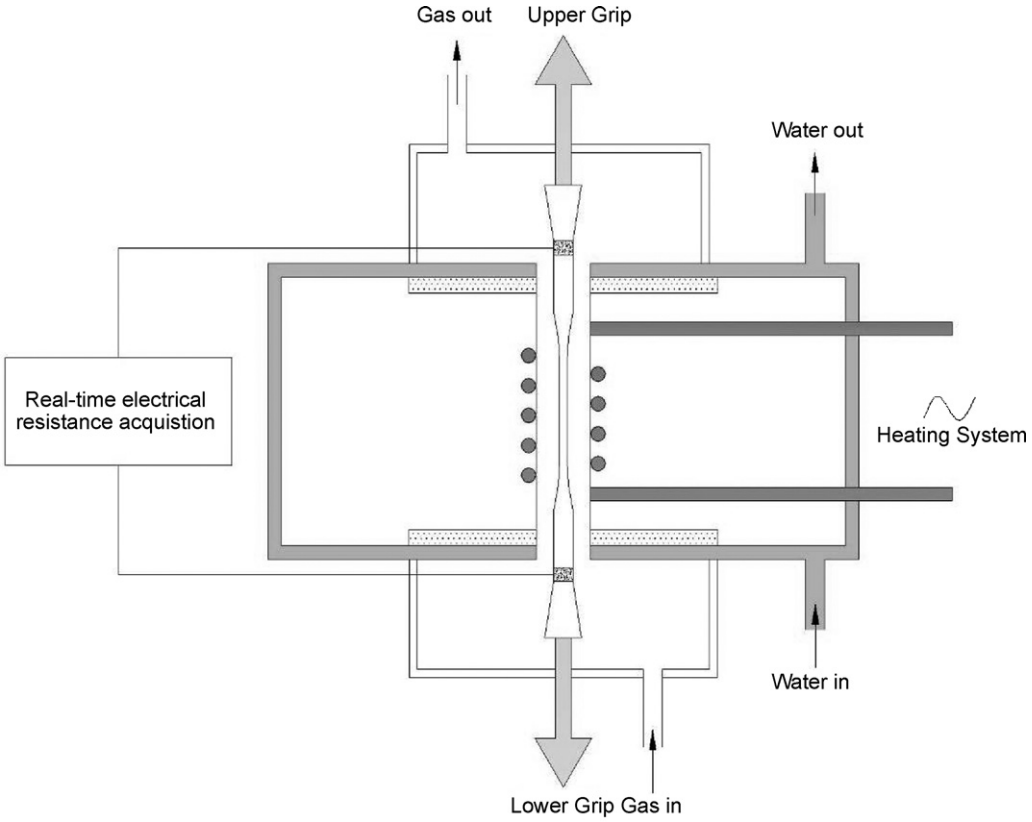

Fig. 2. Schematic of test equipment and specimen setup.

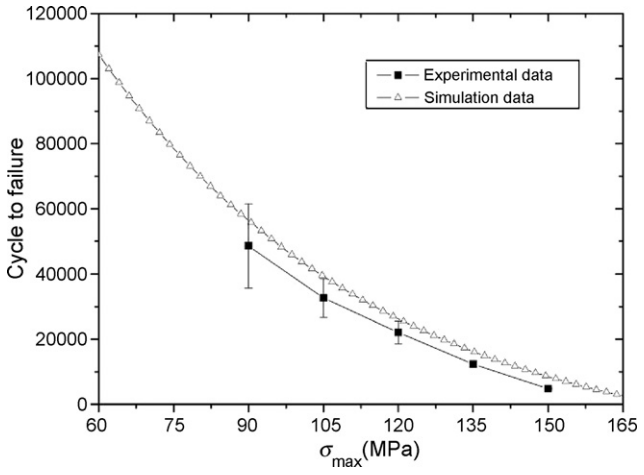

Fig. 3. Comparison between experimental and simulation life of fatigue-stressed oxidation experiment.

which will lead to more extensive mechanical damage, it can be deduced that the lifetime at high temperature is also lower than that at room temperature.

3.2. Electrical resistance and modulus responses

The basic failure mechanisms most commonly observed in fatigue of fibre-reinforced ceramic matrix composites, including C/C composites, are matrix cracking, fibre/matrix debonding, fibre breakage and carbon phase burn-out, which will cause modulus degradation and electrical resistance variation.

The relationship between the specimen resistance and cycle number was plotted in Fig. 4. As fatigue-stressed oxidation test proceeded, the specimen resistance appeared a slight drop (up to 300th cycle) and followed by a continuous increase until failure. The specimens fatigued at different stresses have similar resistance responses. These changes in electrical resistance occurring during uniaxial loading are known to be attributed to two separate effects as follows[11]: (i) the changes in resistance due to the changes in dimensions of the fibres owing to elastic strain and (ii) the changes in resistance caused by fibre fracture or other changes in the network of touching fibres, this is also contributed by oxidation of the carbon phase. The alignment of the fibres along the load-bearing direction is thought to be responsible for the initial resistance drop. It is also noted that the resistance increased drastically in the last period of specimen life, which is suggested to be the result of fast shrinking core effect and massive fracture of reinforcing fibres. The resistance responses of the specimens tested at other stresses presented the similar phenomenon.

Throughout each test, secant modulus E_S of the specimen was monitored as a function of cycles. Here, E_S is calculated by

$$E_s = \frac{\sigma_{max} - \sigma_{min}}{\varepsilon_{max} - \varepsilon_{min}} \quad (1)$$

The changes of modulus at different stresses are shown in Fig. 5. Compared with Fig. 4, it will be seen that the changes in modulus reflect the changes in electrical resistance taking place at the same period in the test. An initial decline in modulus after the start of cycling occurs at the same period as an increase in resistance. There is next a relatively long plateau period, with little change in modulus or resistance, followed by a rapid reduction in modulus as final failure is approached. From the above discussion, modulus degradation of the composite could be reflected by electrical resistance rise. It has been shown that it is possible to employ resistance measurement as an in situ damage evolution indicator.

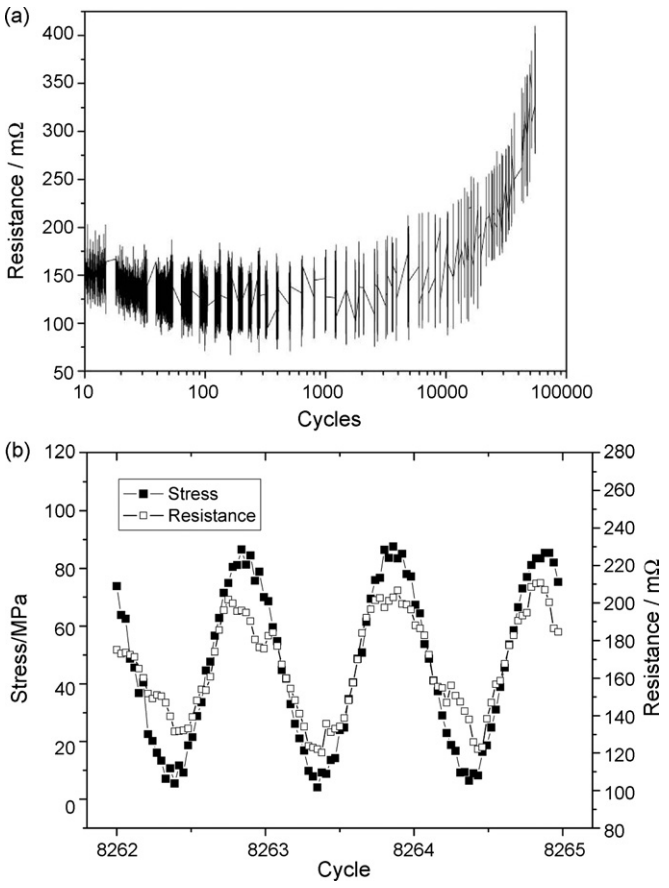

Fig. 4. (a) Electrical resistance response of a specimen fatigued at peak stress of 90 MPa and (b) a magnified view of the abscissa scale.

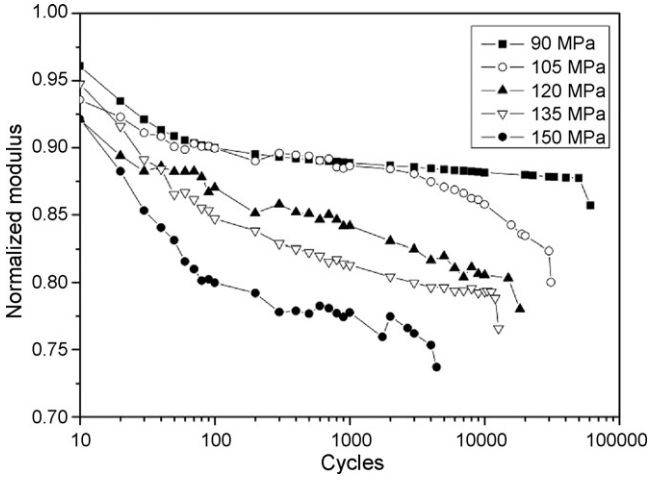

Fig. 5. Modulus responses of C/C composites fatigued at different peak stresses.

3.3. Microstructural damage

SEM micrographs of the polished SiC coating before and after tests are shown in Fig. 6. It is seen from Fig. 6(a) that there are cracks within the coating before tests, which was caused by the different coefficient of thermal expansion (CTE) between the SiC coating and the C/C substrate after processing of the coated composite. The defects shown in the micrographs are caused by the two-dimensional braiding process. Since the whole C/C surface is covered by chemical vapor deposited SiC, the braiding-defect has little contribution to the gaseous diffusion.

After fatigue-stressed oxidation tests, more cracks appeared on the coating, most of which were perpendicular to the loading direction (see Fig. 6(b)). Once the SiC-coated C/C composite was loaded, the C/C substrate was stretched along the loading axial, while the brittle SiC coating could only craze. The width of the cracks is higher when the applied stress is greater, and thus the oxidizing gaseous species diffuse faster into the C/C substrate.

The typical fracture section of the specimen fractured during cyclic loading is shown in Fig. 7. Fig. 7(a) shows the oxidation morphology beneath the SiC coating. Clear fibre oxidation can be observed. Fig. 7(b) shows the near-centre region morphology of the fracture section, where oxidation is negligible. These kinds of microstructural morphologies are mainly caused by the diffusion controlled oxidation kinetic.[12] The carbon is very reactive at the present experiments and consumes oxygen as soon as it is supplied so that the interior becomes deprived of oxygen. A shrinking core effect is seen as the reaction front moves inward.

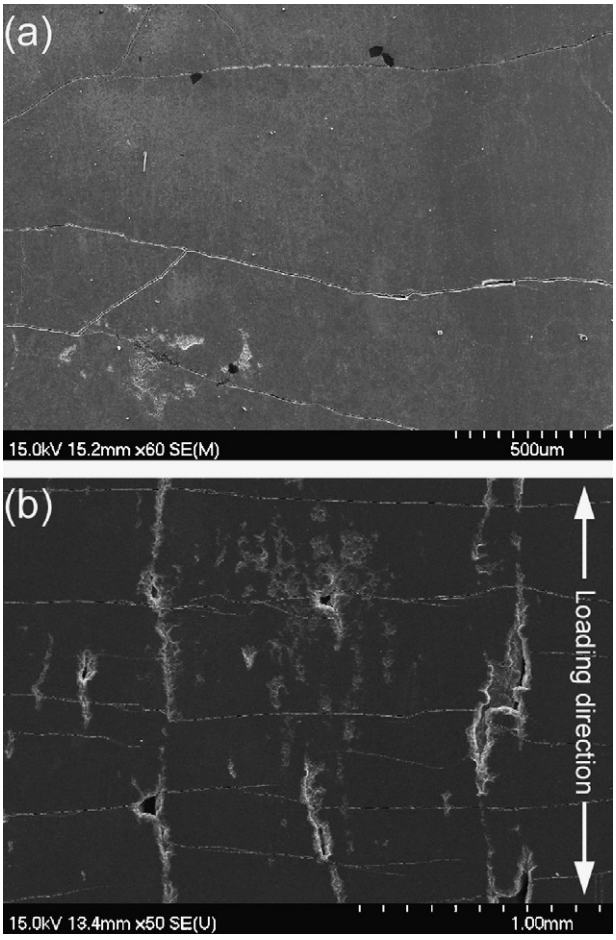

Fig. 6. Cracks of the SiC coating (a) before and (b) after test.

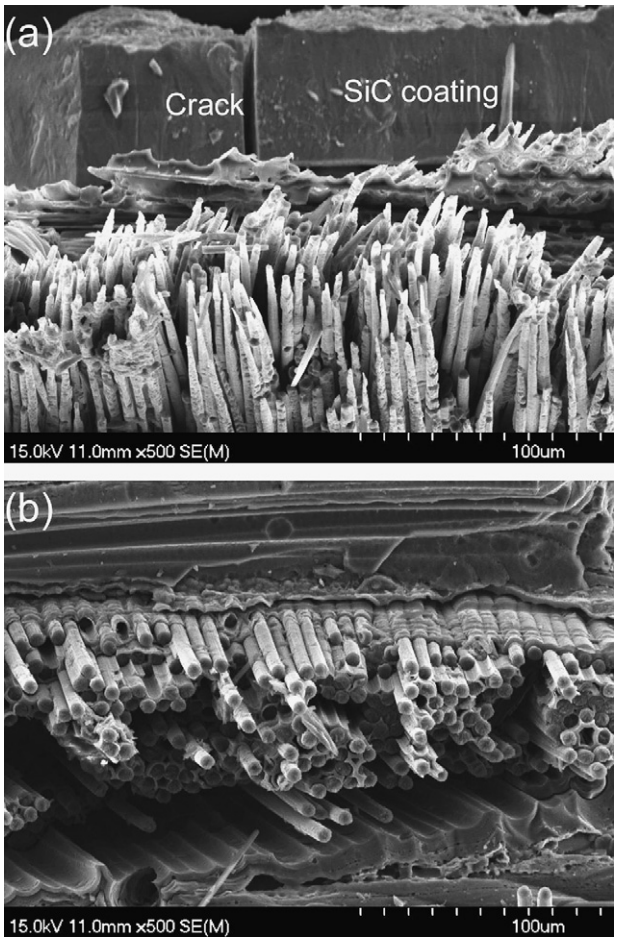

Fig. 7. (a) Superficial oxidation morphology of the fracture section. (b) Centre region of the fracture section.

There will be a sharp gradient in oxygen concentration that is high at the edge where it first diffuses inward and is very low or zero at the carbon surface. Fig. 8(a) shows the position of the reaction front at the time of failure, which occurred during a fatigue-stressed oxidation test. The already consumed side of the reaction front will have a steeply decreasing gradient in oxygen concentration up to the carbon surface while the unconsumed side of the reaction front is deprived in oxygen. In Fig. 8(b), fibre/matrix removal by oxidation can also be observed. Due to the similar crystalline structure between the fibre and interface, oxidation rate difference is neglected in the modeling section.

4. Modeling

4.1. Failure criterion of fatigue-stressed oxidation

As mentioned, the damage process is related to the oxidation and accelerated by the applied loading. In this section, theoretical

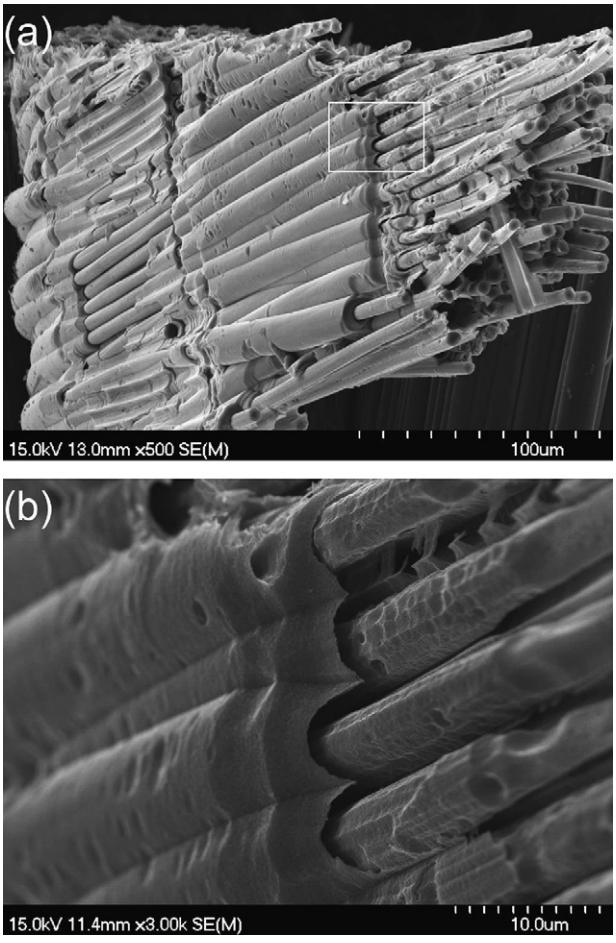

Fig. 8. (a) Oxidation morphology of a fibre bundle showing the reaction front and (b) a magnified view.

calculation is conducted to predict the lifetime on the basis of oxidation of the C/C substrate.

From the discussions in Section 3.1, it is derived that the oxidation of the C/C composite is a gaseous diffusion-controlled process. For diffusion-controlled kinetics, oxidation along microcracks within fibre tows deep into the material is neglected. Composite shrinking core effect is considered to be the main failure mechanism. For convenience, the specimen cross section is set to be a circle. As shown in Fig. 9, after t seconds of fatigue-stressed oxidation, the radius of oxidation cavity is r.

When the composite approaches the critical state of failure, the following equation is satisfied:

$$\frac{S_0}{S_t} = \frac{\sigma_0}{K\sigma_{\max}} \tag{2}$$

where $S_0 = \pi R^2$ is the initial cross section area, $S_t = \pi(R-r)^2$ is the effective load bearing cross section area after t seconds, $\sigma_{\max}$ is the peak fatigue stress, and K is the stress intensity factor in fatigue. It can be explained that a critical radius can be deduced from Eq. (2), which is discussed in the following section.

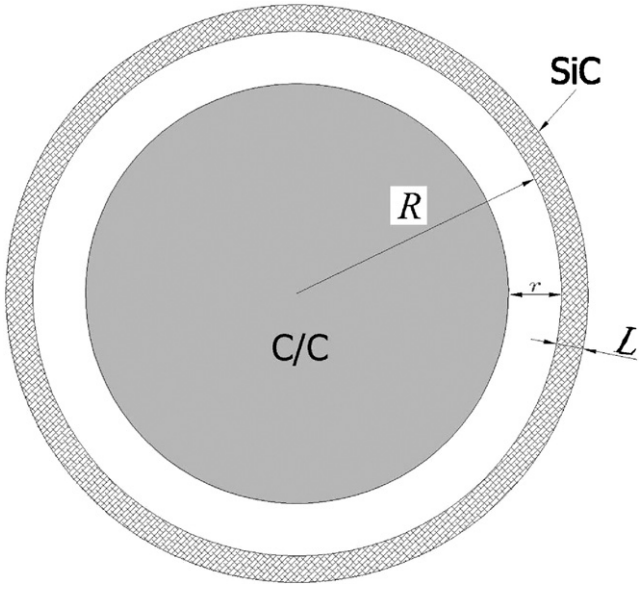

Fig. 9. Schematic of the C/C cross-section after t seconds of fatigue-stressed oxidation.

4.2. Half-cylinder oxidation model

Without considering the effect of applied stress, the oxidation processes of C/C substrate are

(1) Diffusion of gaseous oxidizing species inward through the cracks in the SiC,
(2) Oxidation of cracks walls to form SiO_2,
(3) Oxidation of C/C, i.e. matrix, fibres and fibre/matrix interfacial recession,
(4) Diffusion of CO outward through the cracks in the SiC.

Based on the above kinetics, Jacobson *et al.*[6] developed a half-cylinder oxidation model (see Fig. 10) for SiC-coated C/C. The consumption of carbon is calculated by the following

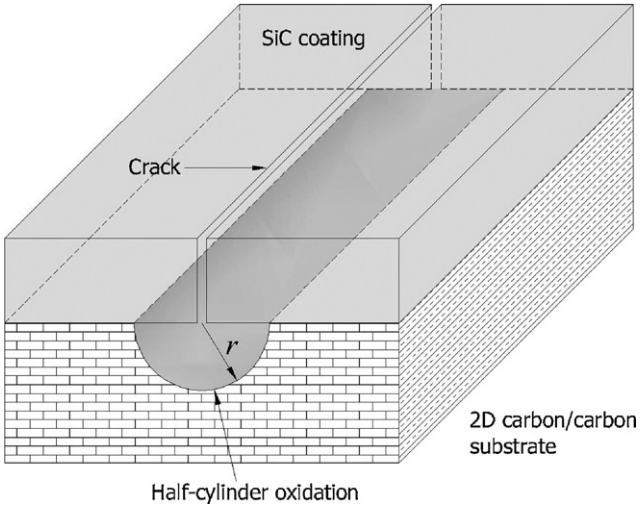

Fig. 10. Schematic of the half-cylinder oxidation pattern of SiC-coated C/C.

equation[6]:

$$\frac{dW_C}{dt} = \frac{M_C D P w l}{R' T L[1-(x_f/L)]} \quad (3)$$

where W_C is the weight loss of carbon (including matrix and fibre), M_C the molecular weight of carbon (12 g/mol), R' the gas constant, w the SiC crack width, l the SiC crack length, D the diffusivity of gaseous oxidizing species, P the partial pressure of gaseous oxidizing species, L the crack depth and x_f is the constant with temperature.

In this model, the oxidation cavity is half-cylinder shaped, thus the weight loss of carbon can also be calculated by

$$\frac{dW_C}{dt} = \rho\frac{dV}{dt} = \rho\left[\frac{d(\pi r^2 l/2)}{dt}\right] \quad (4)$$

Equating (3) and (4) and solving for r results in

$$r = \sqrt{\frac{2M_C D P w t}{\pi\rho R' T L[1-(x_f/L)]}} \quad (5)$$

It is seen from Eq. (5) that at a given temperature, the crack width w is the key variable influencing the oxidation depth r.

4.3. Calculating the crack width w

In the present experiments, crack width w is affected by the temperature T and the applied loading σ. Assume that $w_{T,t}$ is the crack width at temperature T and at time t, which can be calculated by

$$w_{T,t} = w_T + \Delta w_t \quad (6)$$

where w_T is the crack width at temperature T without loading, Δw_t is the increase of crack width caused by the applied stress at time t. w_T can be readily given by

$$w_T = \Delta\alpha(T_P - T)s \quad (7)$$

Here $\Delta\alpha$ is the difference between the CTE of SiC coating and that of the C/C substrate, s is the mean crack spacing and T_P is the SiC coating processing temperature (~1100 °C).

Once the tensile fatigue stress is applied to the specimen, the composite will elongate along the loading direction, while the brittle SiC coating will craze and the already existing cracks will widen. The increase of crack width caused by tensile stress is

$$\Delta w_t = s\frac{\sigma}{E_t} \quad (8)$$

where E_t is the composite modulus at time t. Due to the fatigue stress, matrix cracking, fibre fracture, fibre/matrix interfacial debonding and slipping within the C/C composite can occur, causing modulus reductions, which is proved in Section 3.3. The relationship between the modulus reduction and peak fatigue stress of 2D woven composite can be expressed by [13]

$$-\frac{1}{E_0}\frac{dE_t}{dN} = A\left[\frac{\sigma_{max}^2}{E_0^2\left[1-(E_t/E_0)\right]}\right]^n \quad (9)$$

where N is the cycle number, $N = ft$. A and n are constants. Then, one can first obtain the crack width $w_{T,t}$ at t with given stress and temperature by Eqs. (6)–(9), and by substituting in $w_{T,t}$ terms of w in Eq. (5), the lifetime of the composite can be finally calculated by Eq. (2).

4.4. Comparison of simulation to experiment

The simulation results are plotted in Fig. 3 in hollow triangle dots. A comparison of simulation to experiment indicates the effectiveness of the model. It is important to note that $T > T_P$, according to the model, the coating crack will keep closed when the peak fatigue stress is not sufficiently high, thus the specimen will never fail. In real experiments, the SiC will react with the oxidizing atmosphere

$$SiC(s) + 3H_2O(g) = SiO_2(s) + CO(g) + 3H_2(g) \quad (10)$$

$$2SiC(s) + 3O_2(g) = 2SiO_2(s) + 2CO(g) \quad (11)$$

Water vapor may further react with silica and forms SiOH group, which interrupts the SiO_2 network. The destroyed SiO_2 network makes water vapor diffuse more quickly into the C/C substrate and oxidize the matrix and fibres, the specimen will finally fail. Therefore, when the applied stress is higher (sufficient to open the coating cracks), the simulation data will be closer to experimental results.

The scatter in the life data increased significantly as the peak fatigue stress was lowered. The scatter approached two orders of magnitude greater at a peak stress of 90 MPa than that at 150 MPa. Practically, neither the spacing nor the width of the coating crack is uniform before testing. The scatter in composite life at low applied stress was mainly caused by the inhomogeneity of coating cracks. At higher stresses, the crack width is more dominated by Δw_t, which is controlled by the stress level, thus the degree of scatter becomes lower.

5. Conclusions

For the SiC-coated C/C composite, oxidation of the carbon matrix and fibre and matrix/fibre interface are the dominant damage mechanisms in fatigue-stressed oxidation tests. The higher the applied fatigue stress, the shorter the composite life. A model was developed based on the half-cylinder oxidation pattern. A fatigue-stressed oxidation failure criterion was presented. The SiC coating crack width was found to be the key variable affecting the composite life. Simulations were conducted on the basis of this model, and the results agreed with the experimental data fairly well, although the models do have its limitations.

Acknowledgements

The financial support from Natural Science Foundation of China (Contract No. 90405015) and National Young Elitists Foundation (Contract No. 50425208) is highly acknowledged by the authors.

References

1. Jacobson, N. S. and Curry, D. M., Oxidation microstructure studies of reinforced carbon/carbon. *Carbon*, 2006, **44**, 1142–1150.
2. Zhu, Q. S., Qiu, X. L. and Ma, C. W., Oxidation resistant SiC coating for graphite materials. *Carbon*, 1999, **37**, 1475–1484.
3. Huang, J. F., Zeng, X. R., Li, H. J., Xiong, X. B. and Fu, Y. W., Influence of the preparation temperature on the phase, microstructure and anti-oxidation property of a SiC coating for C/C composites. *Carbon*, 2004, **42**, 1517–1521.
4. Fu, Q. G., Li, H. J., Shi, X. H., Li, K. Z. and Sun, G. D., Silicon carbide coating to protect carbon/carbon composites against oxidation. *Scripta Mater.*, 2005, **52**, 923–927.
5. Zeng, X. R., Li, H. J., Yang, Z. and Kang, M. K., Investigation of microstructure for oxidation protection coated C/C composites. *Trans. Met. Heat Treat.*, 2000, **21**, 64.
6. Jacobson, N. S., Leonhardt, T. A., Curry, D. M. and Rapp, R. A., Oxidative attack of carbon/carbon substrates through coating pinholes. *Carbon*, 1999, **37**, 1411–1419.
7. Lamouroux, F., Naslain, R. and Jouin, J. M., Kinetics and mechanisms of oxidation of 2D woven C/SiC composites: II, theoretical approach. *J. Am. Ceram. Soc.*, 1994, **77**, 2058–2068.
8. Luan X., Degradation mechanisms and life prediction of 3D C/SiC composite in high temperature environments including oxidizing gas and stress. PhD Thesis, Northwestern Polytechnical University, Xi'an, China (2007), Chapter II, 33–35.
9. Goto, K., Hatta, H. and Katsu, D., Tensile fatigue of a laminated carbon–carbon composite at room temperature. *Carbon*, 2003, **41**, 1249–1255.
10. Goto, K., Furukawa, Y. and Hatta, H., Tensile fatigue of 2D carbon–carbon composite at room temperature. *Compos. Sci. Technol.*, 2005, **21**, 1–8.
11. Irving, P. and Thiagarajan, C., Fatigue damage characterization in carbon fibre composite materials using an electrical potential technique. *Smart Mater. Struct.*, 1998, **7**, 456–466.
12. Halbig, M. C. and Cawley, J. D., Modeling the Environmental Effects on Carbon Fibres in a Ceramic Matrix at Oxidizing Conditions. NASA Report, 2000, NASA/TM—2000-210223.
13. Karandikar, P. G. and Chou, T. W., Damage development and moduli reductions in Nicalon–calcium aluminosilicate composites under static fatigue and cyclic fatigue. *J. Am. Ceram. Soc.*, 1993, **76**, 1720–1728.